Biomass Conversion and Biorefinery (2021) 11:2947–2961
https://doi.org/10.1007/s13399-020-00672-7

ORIGINAL ARTICLE

The characterisation of biochar and biocrude products of the hydrothermal liquefaction of raw digestate biomass

Oseweuba Valentine Okoro [1,2] · Zhifa Sun [2]

Received: 5 December 2019 / Revised: 10 February 2020 / Accepted: 5 March 2020 / Published online: 29 April 2020

Abstract

The ease and simplicity of applying the anaerobic digestion technology in the generation of cheap bioenergy has led to its global acceptance as a viable technique for simultaneous value extraction from high moisture containing waste biomass and organic waste management. Crucially, however, the widespread application of anaerobic digestion technologies results in the associated generation of large masses of raw biogas digestate, leading to unintended digestate management challenges. A previous study subsequently investigated the utilisation of the digestate as a sustainable feedstock for bioproduct generation via the incorporation of the hydrothermal liquefaction (HTL) technology. As a sequel to the aforementioned study, the present work sought to investigate the characteristic properties of the major products of the hydrothermal liquefaction processing of anaerobic digestate while simultaneously proposing viable and practical uses of these products. Several characterisation techniques such as nuclear magnetic resonance spectroscopy, Fourier transform infrared spectroscopy, inductively coupled plasma mass spectrometry and gas chromatograph-mass spectrometry were applied with representative HTL products from digestate employed in this regard.

Keywords Hydrothermal liquefaction · Biochar · Biocrude · Waste management · Biorefinery

1 Introduction

In line with the recent upsurge of the interest in exploration of value extraction opportunities using freely available organic waste streams, the anaerobic co-digestion of hydrolysed dissolved air flotation (DAF) sludge and the meat processing stockyard waste was assessed as a viable pathway for organic waste management via its utilisation in the generation of useful bioenergy in form of biogas [1]. However in addition to the biogas product generated, large masses of raw digestate residues are also produced at the conclusion of anaerobic digestion processes [1–3]. These large masses of raw digestate are suggested to retain harmful zoonotic agents that may cause infections in both humans (i.e. influenza disease) and livestock (i.e. foot and mouth disease) [4, 5]. For countries where the magnitude of environmental impact associated with such organic streams constitutes a primary concern, the digestate must be treated prior to its disposal. Exploring existing technologies employed in *raw* digestate management, hydrothermal liquefaction was proposed as a possible technology that may facilitate digestate sterilisation, due to the high temperature (250–370 °C) and pressure conditions (4–22 MPa) typically imposed and value extraction, while circumventing the need for initial dewatering/drying operations [6]. Preliminary studies subsequently showed that the unit processing cost for *raw* digestate may range from US$271.7/ton (a year 2014 study) [7] to US$482.1/ton (a year 2018 study) [8]. These unit processing costs are high compared to the estimated unit processing cost of *raw* digestate of US$77/ton [8] when the alternative one-step hydrothermal liquefaction (HTL) process is employed. Experimental investigation of HTL of raw digestate was therefore justified to assess the possibility of recovery of valuables from raw digestate. A previous study therefore investigated the utilisation of the HTL process for value extraction from the high-moisture *raw* digestate feedstock [8, 9]. Digestate sterilisation due to the high conditions of temperature and pressure was anticipated, as stated earlier above. This previous study served to demonstrate that value extraction from wet

✉ Oseweuba Valentine Okoro
oseweuba@sun.ac.za

✉ Zhifa Sun
zhifa.sun@otago.ac.nz

[1] Department of Process Engineering, Stellenbosch University, Private Bag X1. Matieland, Stellenbosch 7602, South Africa

[2] Department of Physics, University of Otago, PO Box 56, Dunedin, New Zealand

Published online: 29 April 2020

digestate biomass in the absence of preliminary energy intensive and costly drying operations was functional. Initial investigations presented in [8, 9] also established that useful streams of specifically biochar and biocrude could be generated via hydrothermal liquefaction processing of digestate (moisture content ~ 97 wt%) as presented in Fig. 1.

It must be stated that although the yield of the biocrude product was determined to be low at ~ 7 wt% db (dry weight basis) in our previous work [8, 9], it was comparable to yields reported in other HTL studies involving high moisture feedstocks. For instance in the studies of [10] and [11], the biocrude yields from the HTL of sludges were reported to be 8% and 9.4%, respectively, on a dry weight basis. These poor biocrude yields suggest that the proposed HTL of anaerobic digestate will be more valuable if proper uses of the product streams are established via undertaking an extensive characterisation of the unique product streams. Indeed the higher yield of the associated biochar (~46% dry weight basis) and the possibility of digestate sterilisation may better justify the HTL processing of digestate [8, 9]. The present paper therefore seeks to provide an exhaustive assessment of the useful products of HTL of *raw* digestate while also proposing logical applications for the utilisation of the product streams based on their characterisation results. The novelty of the present study is emphasised by its dualistic focus on the characteristics and practical applications of the HTL products obtained from a high moisture raw digestate. It must also be stated that at the time of writing this paper, no study exists in the literature in which digestate-sourced HTL products were extensively studied and characterised as a precursory step to suggesting their specific practical uses as biofuels, biomaterial, etc.

2 Materials and methods

The biocrude, biochar and HTL -gas samples were obtained via HTL of the digestate feedstock, using methods described in [8, 9]. The digestate feedstock is composed of elemental carbon, hydrogen, nitrogen, oxygen and ash content on a dry weight basis of 28.64%, 4.45%, 2.8%, 24.6% and 39.53%, respectively, with negligible sulphur content [1]. The biochar and biocrude products have been identified as the most valuable products. These optimally produced products [9] have been specified as typical (representative) products (TPs) in the present study to simplify the analysis. The product of post-HTL water, has not been analysed further in the present study since its characteristic low (less than 1%, mass basis) concentration of any components of value, discourages the incorporation of further energy intensive and costly analysis steps. Crucially, however, the present study recognises the possibility of employing the post-HTL water as a feedstock for secondary H_2 production via microbial electrolysis or as a nutrient source for microalgae cultivation [8]. Future work in the area will therefore seek to explore the suitability of post-HTL water for the aforementioned uses.

The methods employed in characterising the biocrude, biochar and HTL-gas products are extensively described below. All experiments reported have been conducted in duplicate with mean values reported.

2.1 Elemental analysis of the TP of biochar and the biocrude product from digestate

Elemental analysis of the TP of biocrude and biochar from the HTL of digestate was undertaken using the Carlo Erba EA1108 elemental analyser (FISONS, Milan, Italy) to determine the carbon, nitrogen, sulphur and hydrogen content. The ash content of the biochar was determined according to the ASTM D 2017-98 standard method [12]. Based on the carbon content, the biochars are broadly classified into: class 1 (carbon content ≥ 60 wt%), class 2 (carbon content, 30–60 wt%) and class 3 (carbon content, 10–30 wt%), which represent biochars with high energy density, moderate energy density and low energy density, respectively [13]. The oxygen content was measured using the ASTM D 3176-15 standard method [14, 15]. The higher heating value ($HHV_{biocrude}$) of the

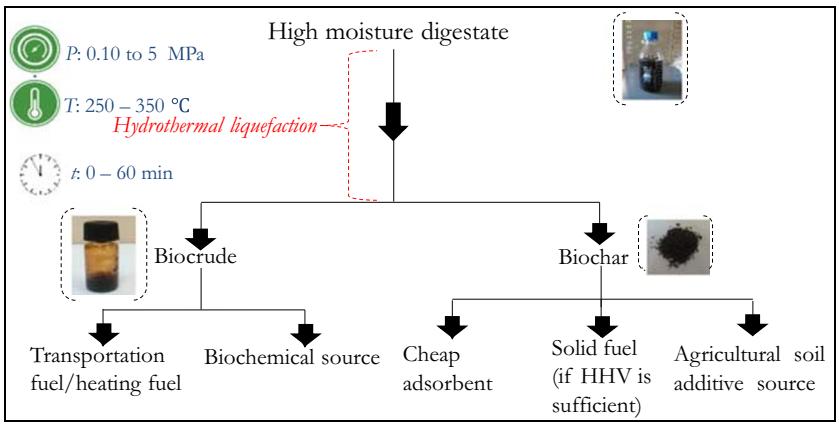

Fig. 1 Hydrothermal liquefaction of anaerobic digestate

biocrude and the higher heating value ($HHV_{biochar}$) of biochar, both in MJ/kg, were subsequently determined using Eq. 1 [11] and Eq. 2 [16], respectively.

$$HHV_{biocrude} = 0.338\mathrm{C} + 1.428\left(\mathrm{H} - \frac{\mathrm{O}}{8}\right) + 0.095\mathrm{S} \quad (1)$$

$$HHV_{biochar} = 0.3491\mathrm{C} + 1.1783\mathrm{H} + 0.1005\mathrm{S} - 0.1034\mathrm{O} - 0.0151\mathrm{N} - 0.0211\mathrm{A} \quad (2)$$

where C, H, S, O, N and A represent the content of carbon, hydrogen, sulphur, oxygen, nitrogen and ash in mass percentages, respectively.

To amplify compositional similarities between the biocrude/biochar and fossil fuels, a Van Krevelen diagram was utilised [17, 18]. For clarity, a Van Krevelen diagram is a plot of H/C ratio as a function of O/C ratio [19]. Compositional similarities highlighting the level of carbonisation were efficiently presented using a Van Krevelen diagram [20]. Generally, lower H/C and O/C ratios are indicative of a higher level of carbonisation. In this study, comparative assessments were therefore undertaken to explore elemental compositional similarities between biocrude, biochar, fossil fuels and unprocessed biomass from agricultural sources. The relevant H/C and O/C data for several biomass (agriculture residue) feedstocks have been obtained from literatures.

2.2 Assessment of the representative biocrude as a biochemical mixture

The compositional assessment of biocrude was achieved using traditional methods presented in the literature. These methods are specified as nuclear magnetic resonance (NMR), Fourier transform infrared (FTIR) and gas chromatograph-mass spectrometry (GC-MS) assessment methods [11, 17, 21–24]. The NMR and FTIR methods provide preliminary functional group information without providing individual molecular-level information via an analysis of the distribution of resonating protons of functional groups and the distribution of chemical shifts due to the vibration of bonds of functional groups, respectively [11]. The NMR and FTIR analysis methods are recognised as necessary for initial compositional assessments of biocrude, thus providing an indication of all possible compounds that may be present based on crucial functional group information. The GC-MS method enables the tentative identification of the main chemical compounds present via the comparative assessment of the mass spectral of fragmentation patterns generated and the mass spectral database of the National Institute of Standards and Technology (NIST) [11, 17]. The methods of NMR, FTIR and GC-MS are identified as sufficient when utilised simultaneously, as these methods are capable of complementing each other, thus providing a sufficient basis for a comprehensive description of the digestate-sourced biocrude sample.

2.2.1 Characterisation of biocrude by proton nuclear magnetic resonance

A mass of 40 mg of the biocrude sample was dissolved in 600 μL of deuterated chloroform ($CDCl_3$) (Sigma-Aldrich, Auckland, New Zealand), and solution samples were loaded to a Varian 500 MHz NMR system using a sample probe and an A7620-AS automated NMR sample changer (Agilent, USA). A solution with a concentration of 0.03% v/v of tetramethylsilane (TMS) in the $CDCl_3$ was utilised as an internal standard. The ^{1}H NMR spectra of the biocrude sample were acquired at 500 MHz with a pulse delay of 4 s, a 60° pulse angle, a spectral width of 16 ppm and 32 scans per ^{1}H spectrum. The chemical shifts σ, measured in ppm, associated with different resonating protons in specific functional groups were analysed using the MestReNova software, and the proton percentage distribution is calculated. The results were presented in terms of the proton percentage distribution according to the chemical shifts of the respective resonating protons. The major functional groups present have been identified based on the proton percentage distribution and explained using the categorisation methodology applied in previous biocrude studies [25–27]. The categorisation methodology involves specifying and grouping the functional groups present according to the standard chemical shift ranges detected [25–27]. The categorisation methodology constitutes the preferred method employed in the literature to analyse ^{1}H NMR results of the biocrude product due to its complexity [25].

2.2.2 Characterisation of biocrude by Fourier transform infrared

A mass of 30 mg of biocrude was applied to an attenuated total reflection (ATR) crystal surface after initial background scans of the dry surface at a temperature of 25 °C and had been conducted to ensure surface purity. Spectra signals were collected from wavelengths ranging from 400 to 4000 cm^{-1} at a resolution of 4 cm^{-1} and averaged over 32 replicate scans. The spectral analysis was achieved using the OPUSTM software (Bruker Optik, Ettlingen, Germany). Major wave numbers (cm^{-1}) generated were compared with standard wavenumber bands associated with specific functional groups. Only major wave numbers (cm^{-1}) generated were considered since significant overlaps in wave numbers are expected from the FTIR spectral signals obtained from the biocrude sample due to its complexity. The standard wavenumbers associated with specific chemicals have been obtained from the literature [28, 29].

2.2.3 Characterisation of biocrude by gas chromatography-mass spectrometer

The GC-MS analysis was achieved using an Agilent 5890 N series II equipment coupled to a mass selective detector (MSD), model 5973 (Agilent Inc., California, USA). The

separation of the biocrude into its component molecules was achieved using an H-P 5MS GC column (length, 50 m; internal diameter, 0.32 mm; film thickness, 1.05 μm) with the column head pressure maintained at 88.25 kPa. Hydrogen was utilised as the carrier gas at a flow rate of 1.2 mL/min.

Dissolved in dichloromethane at a concentration of 1 wt%, 1 μL of biocrude was injected into the column in a split-less mode. The oven temperature was subsequently programmed as follows: 170 °C maintained for 5 min, 4 °C/min ramped to 200 °C, held constant at 200 °C for 3 min, 4 °C/min ramped to 290 °C, held constant at 290 °C for 1 min, 20 °C/min ramped to a final temperature of 325 °C and was held constant for 15 min. The major separated molecules present in the biocrude were indicated by the major GC-MS peaks, and the molecules identified using the mass spectrometry database of the National Institute of Standards and Technology (NIST). Molecule quantitation was carried out in a total ion chromatogram (TIC) mode. In the present study, the relative abundance of each major compound identified was reported in terms of their respective percentage peak areas relative to the total area of the major peaks. This approach was employed since previous studies in the research area [30–33] previously represented the abundance of chemical components in a similar way.

2.3 Assessment of the representative biocrude as a liquid fossil fuel alternative

To enable an initial assessment of the biocrude as a petroleum (crude) fuel alternative, the values of HHVs and °API gravities of the biocrude sample were compared with those of petroleum fuel fractions [34, 35]. The HHVs of biocrude and petroleum fuel fractions were compared since HHV is widely known as an important parameter that dictates the energy content of fuels [36]. Their °API gravities were also compared since the parameter constitutes the single most important quality defining characteristic of petroleum fuel fractions [37]. The °API gravity serves as an indicator of the proportion of light and middle distillates obtainable from a distillation process [37] and is also related to the oil viscosity property [38]. The °API gravities of different fractions of petroleum fuel oil are presented in Table 1.

The °API gravity of the digestate sourced biocrude was estimated as follows [34, 39, 40]

$$^{\circ}\mathrm{API} = \left(\frac{141.5}{\mathrm{S.G}_{60^{\circ}\mathrm{F}}}\right) - 131.5 \tag{3}$$

where

$$\mathrm{S.G}_{60^{\circ}\mathrm{F}} = \mathrm{S.G}_{t^{\circ}\mathrm{F}} + \left[3.31 \times 10^{-4} \times (t^{\circ}\mathrm{F} - 60^{\circ}\mathrm{F})\right] \tag{4}$$

$\mathrm{S.G}_{60\ ^{\circ}\mathrm{F}}$ is the specific gravity of petroleum fuel and biocrude at 60 °F (16.56 °C) and 1 atm; $\mathrm{S.G}_{t\ ^{\circ}F}$ is the specific gravity of biocrude measured at room temperature of 71.6 °F (22 °C) and pressure of 1 atm. $\mathrm{S.G}_{t\ ^{\circ}F}$ of the biocrude at room temperature of 71.6 °F was measured using the ASTM D70-03 methods [41].

Table 1 Major fractions of petroleum fuel oil

Categorisation	Specification
Light	°API gravity > 31.1
Medium	22.3 < API gravity < 31.1
Heavy	10 < °API gravity < 22.3
Extra heavy	°API gravity < 10.0

2.4 Assessment of the representative biochar as an agricultural soil enhancer

In line with the objectives of this study, the properties of the biochar product as an agricultural soil enhancer were assessed. These properties include stability as a measure of the recalcitrance of the biochar matrix [20], pH, electrical conductivity [42] and morphology [43]. In the present study, similar experiments were undertaken using digestate to provide a basis for comparisons and discussions. For emphasis both (dried) digestate and (dried) biochar samples have been initially finely ground and sieved using an Endecott meshes of 300 and 230 (Endecott, Sydney, Australia) to ensure the particle size, x, of digestate and biochar employed were comparable at 0.048 mm < x < 0.063 mm. Additional experiments to assess the mineral composition of the biochar production were also undertaken as an *indicative* measure of future suitability as a nutrient source for soil [14].

2.4.1 Thermal stability assessment of biochar based on thermal gravimetric analysis (TGA)

According to Rutherford et al. [44], the presence of recalcitrant carbon in biochar will have crucial effects not only on its carbon storage potential but also on the long-term stability of the soil to which it is applied. The stability of biochar is a measure of its ability to resist deterioration over time thus avoiding possible release of unwanted greenhouse gas of CO_2 [45]. In other words, the longer biochar is retained in the soil the longer its potential positive benefits on agricultural soil properties are made available [45]. One way of testing the stability of the biochar product is via the determination of the thermal lability using the results of TGA assessments as follows [46:

$$Th_l = \frac{\Delta m_{350-550^{o}C}}{\Delta m_{110-350^{o}C}} \tag{5}$$

where Th_l is the index of thermal lability where a higher index suggests a higher susceptibility to thermal destruction, $\Delta m_{350-550\ ^{\circ}C}$ is the measured mass loss detected in biochar and

digestate between the temperatures of 350 °C and 550 °C and $\Delta m_{110–350\,°C}$ is the measured mass loss detected in biochar and digestate between the temperatures of 100 °C and 350 °C.

The TGA of the biochar was therefore undertaken. The TGA of the biochar product was performed using a TGA Q50 model thermal analyser (Alphatech, Dunedin). To provide a basis for discussions relating to the thermal stability of biochar, the TGA of the original digestate was also assessed. Briefly, 14 mg of the biochar was introduced to a tared platinum pan of the TGA device. The biochar was then heated in a nitrogen environment and at a nitrogen gas flow rate of 10 mL/min. During the heating process, a linear heating rate of 5 °C/min was initially imposed to raise the biochar temperature from an initial temperature of 30 to 105 °C. An isotherm condition was subsequently imposed for 10 min, and then the temperature was ramped at a rate of 5 °C/min from 105 to 680 °C. Further increments in the temperature were considered unnecessary given that the upper temperature limit of 550 °C was sufficient for thermal lability analysis.

2.4.2 pH value and electrical conductivity assessments of biochar

Other useful properties such as the pH value and the electrical conductivity (EC) of the biochar product were also determined. The pH value is used to assess the capacity of biochar to neutralise unfavourable acidic soils [47], and the EC value is a preliminary indicator of soil health, with a higher EC suggesting the presence of minerals and nutrients in the biochar product which may be available to the soil [48].

Briefly, 1 g of biochar was introduced to 20 mL of deionised water and agitated for 90 min according to the international biochar initiative standard methods [49]. After 90 min, the pH value of the biochar and deionised water mixture was measured using a Hanna precision pH metre, model 209. The electrical conductivity of deionised water is negligible at a value of 5.5 μS/m [50]. After 90 min, the pH value of the biochar and deionised water mixture was measured using the Hanna precision pH metre. The electrical conductivity (EC) of the biochar and deionised water mixture was subsequently determined using a handheld conductivity metre (Eutech Cond^{6+}, Thermo Fisher Scientific, New Zealand).

2.4.3 Morphology assessment of biochar

Surface morphological characteristics of the biochar were also assessed and compared to the morphological characteristics of the original digestate to highlight the effect of hydrothermal liquefaction treatment on surface structure. Initial comparisons were undertaken via simple visual assessment of the images generated using scanning electron microscopy (SEM).

The biochar sample was initially coated with a gold palladium alloy, using an Emitech K575x sputter coater, to a coat thickness of 10 nm. The coated samples were then viewed using a JEOL JSM-6700F field emission scanning electron microscope (JEOL Ltd., Tokyo, Japan) with an accelerating voltage of 5 kV. Images highlighting the morphology of biochar were subsequently acquired.

2.4.4 Mineral content of biochar

The mineral content of digestate-sourced biochar was assessed. This assessment was undertaken to demonstrate the *potential* utilisation of biochar as a sustainable nutrient source for plant growth. This is because previous studies have demonstrated that biochar possesses the capacity to release some of its minerals as nutrients to the soil over time [51, 52]. At this juncture, it is crucial to state that the determination of the mineral content of bio char for its use as a soil additive is largely *indicative*. This is because a practical and undisputed way to demonstrate the viability of biochar's use to enhance soil properties is to introduce the biochar to agricultural soil and assess overall crop growth performance. This is because biochar's impact will depend on several factors such as soil type and characteristics, type of cultivated crop and the state of the mineral (i.e. the state of the mineral of either ion, or element, determines its availability to the crop).

In this study, however, only the mineral content of the biochar product has been assessed. Assessments have been undertaken by determining the concentrations of nitrogen, potassium, phosphorous, sulphur, calcium and magnesium, which are typically macronutrients and the concentrations of iron, manganese, zinc, copper and boron which are typically micronutrients [53–55], present in biochar. The concentrations of sodium and titanium in biochar were also measured because of their roles as potassium substitutes in plant metabolism [56] and role in bio-simulation [57]. Although aluminium is not a crucial nutrient for plant growth [58], its concentration was also measured, because previous studies showed that high concentrations of Al^{3+} ions may lead to plant toxicity effects [59]. The concentrations of nitrogen and sulphur in g per kg of biochar were measured via elemental analysis using a Carlo Erba EA1108 elemental analyser (FISONS, Milan, Italy). The concentrations of nitrogen and sulphur in the biochar were measured using a Carlo Erba EA1108 elemental analyser (FISONS, Milan, Italy). The concentrations of potassium, phosphorous, iron, manganese, zinc, copper and boron were determined using an inductively coupled plasma mass spectrometry system (ICP-MS).

Briefly, a 0.1 g of finely ground biochar was initially introduced in a solution containing 10 mL of (15.8 M) HNO_3 and 1 mL of 30% w/w H_2O_2 in water for 1 h, to initially "dissolve" the biochar for trace metal release. After 1 h, the mixture was transferred to a microwave (MARS6, CEM Corporation, Matthews, NC, USA) at

200 °C for 15 min, to further aid trace metal release. After 15 min, the biochar "solution" was cooled and dried to a volume of 1 mL using a hot plate at a temperature of 90 °C to concentrate the solution. A volume of 0.5 mL of concentrated (22.6 M) HF was introduced to the resulting biochar "solution" and heated at a temperature of 100 °C for 12 h. After cooling, the resulting solution was diluted by weight with 2% v/v HNO_3 solution to a final volume of 5 mL. An Agilent 7900 quadrupole ICP-MS (Agilent Santa Clara, California, USA), equipped with an octopole collision/reaction cell and auto sampler, was used to measure the concentration of trace nutrients present in the biochar solution. Prior to analysis, the solution was diluted to 100 times its volume with 2% v/v HNO_3 into the analytical range of the ICP-MS and subsequently analysed. A blank solution of 2% v/v HNO_3 contains a cocktail of reference elements was also analysed via ICP-MS to test for interferences and error. Calibration solutions were prepared from commercial standards (Agilent Technologies, Santa Clara, CA USA) with NIST traceable certification.

2.5 HTL-gas composition

The gas sample (1 mL) was introduced using an airtight syringe into two separate Agilent 6890 N GC systems via a common manifold with a gas split. Both the GC systems were calibrated with Alpha Class standard mixes. The analysis for the concentrations of H_2, CO_2 and CH_4 was achieved by running the gas mixture through a column of Porapak Q (HP Plot Q + PT; length, 30 m; internal diameter, 0.53 mm; film thickness, 40 μm) and a column of MS5A (HP MS5A; length, 55 m; internal diameter, 0.53 mm; film thickness, 50 μm) on a GC system. The concentrations of the gas sample were subsequently measured using dual thermal conductivity detectors under a temperature ramp (0 °C to 100 °C). Testing for hydrocarbons in the gas mixture was achieved by running the gas through a column of HP-AL/M (alumina) (length, 30 m; internal diameter, 0.53 mm; and film thickness, 15 mm) on another GC system. The concentration of the hydrocarbon components was detected using a flame ionisation detector. Detection of the concentration of trace CO was undertaken via determination of the (increased) concentration of CH_4 after the methanisation of the gas mixture was undertaken. The methanisation of the gas mixture involves the hydrogenation of CO using H_2 gas under the action of Ni-NiO as catalyst. Due to the difficulty of distinguishing between N_2 generated from the HTL process and N_2 employed in achieving the initial HTL reactor pressure condition, gas composition were estimated on a N_2 free basis. This test was conducted, offsite, using the facilities of a commercial laboratory.

3 Results and discussion

3.1 Elemental analysis of representative biochar and biocrude products

Elemental distribution of representative biochar and the biocrude products of HTL processing of digestate were determined. The C, H, N, O and S contents (dry mass basis) of the biocrude product were shown to be 74.7%, 9.34%, 3.17%, 11.51% and 1.29%, respectively. The C, H, N, O, S and A contents (dry mass basis) of the biochar product were shown to be 13.57%, 1.89%, 0.89%, 7.85%, 0.34% and 75.47%, respectively. The empirical formulas of biocrude and biochar on an ash-free basis can therefore be shown to be $C_{77}H_{116}N_3SO_4$ and $C_{51}H_{86}N_3SO_{11}$, respectively. The biochar product is therefore a class 3 biochar product given that its carbon content of 13.57% is between 10 and 30%. The HHV of biocrude and biochar were subsequently determined to be 36.7 MJ/kg and 4.58 MJ/kg, respectively. Based on the elemental distribution, the biocrude and biochar products can be shown to present O/C (H/C) ratios of 0.0173(0.125) and 0.026 (0.139), respectively, as shown in Fig. 2.

Figure 2 also shows that liquid fossil fuels are characterised by O/C and H/C ratios ranging from 0.0012 to 0.01 and 0.12 to 0.17, respectively, and solid fossil fuels (i.e. anthracite and meta-anthracite) are characterised by O/C and H/C ratios ranging from 0.02 to 0.29 and 0.006 to 0.07, respectively. Biomasses of agricultural residues (sugar cane bagasse and corn stalks) and the digestate (used in this study) are characterised by O/C and H/C ratios ranging from 0.77 to 1.00 and 0.12 to 0.16, respectively. It is seen from Fig. 2 that based on the distribution of the elemental ratios, the biocrude and biochar produced from digestate are 'close' to the liquid fossil fuels and 'far away' from the agriculture residues and the digestate, suggesting some compositional similarities with liquid fossil fuels. However, due to the low energy content (HHV) of the biochar product, it can be stated that employing the digestate-sourced biochar as a fuel will not constitute a practical pathway. Additionally, the high ash content

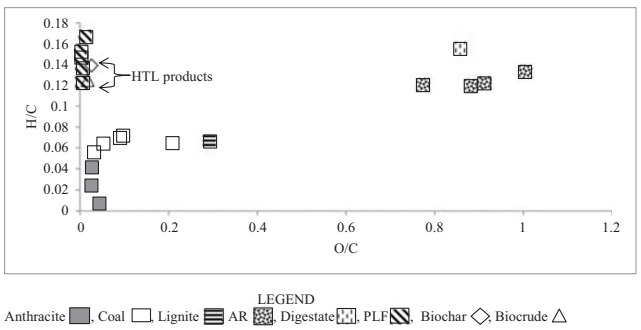

Fig. 2 Van Krevelen diagram (VKD) for compositional assessment of biocrude and biochar relative to fossil fuels and biomass [34, 35, 59–61]

(75.47%, dry mass basis) of biochar implies that its use as a solid fuel will reduce the performance of any environmental pollution control systems, due to the higher possibility of ash deposition during control system operations typically incorporated in biofuel systems [62].

3.2 Major chemical species present in the representative digestate biocrude product

3.2.1 Functional groups detection by proton nuclear magnetic resonance

Based on the ^{1}H NMR analysis conducted, the resonating protons associated with functional groups present in the biocrude product were detected. The ^{1}H NMR output shows that the distribution of the resonating protons can be categorised into groups as highlighted in Table 2. The ^{1}H NMR result shows that based on the categorisations in Table 2, group A, group B, group C, group D, group E and group F, respectively, account for 66.95%, 24.09%, 4.65%, 0.67%, 3.64% and 0% of the total number of resonating protons are present in the digestate-sourced biocrude sample. The high percentage of the resonating protons in group A indicates that the resonating protons, which are attached either to the carbon atoms in saturated compounds (alkanes) [27] or to the carbon atoms that are located at least 2 bonds away from a C=C bond [25], are significantly present in the biocrude product. The functional groups in group B were also shown to constitute the next most dominant group, with the resonating protons detected accounting for 24.09% of the total number of resonating protons present. This suggests that functional groups contain protons that are either attached to carbon atoms directly bonded to a C=C bond or to carbon atoms are located at least 2 bonds away from a heteroatom, of N or O [25]. The bond of C=C may be aromatic or olefinic. The results also suggest the presence of olefins and nitrogenous and oxygenated compounds such as straight or branched amides and N- and O-heterocyclic compounds [26]. Also, the protons associated with the functional groups in group C account for 4.65% of the total number of resonating protons present. Group C specifies the presence of protons directly bonded to carbon atoms attached to an aliphatic alcohol or ether or a methylene group that joins two aromatic rings [25]. The low percentage of resonating protons of 0.67% associated with the functional groups present in group D suggests the negligible presence of carbohydrate-like molecules or aromatic ether molecules. The detected percentage of resonating protons in group E of 3.64% indicates that benzene-like structures are present in the biocrude product. The absence of resonating protons associated with the aldehyde functional group, in group F, indicates the absence of the aldehyde functionalities in the biocrude.

3.2.2 Functional groups detection by Fourier transform infrared

Table 3 lists the detected major peak transmittances from the FTIR analysis of the biocrude. Table 3 shows that major wavenumbers of 2922 cm^{-1}, 2844 cm^{-1}, 1375 cm^{-1}, and 1453 cm^{-1}, highlighting the presence of C–H stretching vibrations and C–H bending vibrations of the CH_3 and CH_2 groups, respectively.

The wave number of 1688 cm^{-1}, highlighting the presence of C=O stretching vibrations was also detected. The presence of the CH_3 and CH_2 groups and the C=O bond suggest the presence of carboxylic acids. Other major wave numbers detected include wavenumbers of 719 cm^{-1} and 891 cm^{-1} which indicate the presence of O–H bending vibrations. This may

Table 2 Chemical shift-based categorisations for biocrude [25–27]

Designation	σ (ppm)	Functional groups present
Group A	0.5–1.5	Functional groups containing protons that are either attached to carbon atoms in saturated compounds or attached to carbon atoms that are located at least 2 bonds away from a C=C bond
Group B	1.5–3.0	Functional groups containing protons that are either attached to carbon atoms directly bonded to the C=C bond or are located at least 2 bonds from a heteroatom (O or N)
Group C	3.0–4.4	Functional groups containing protons directly bonded to carbon atoms attached to either an aliphatic alcohol or ether or a methylene group that joins two aromatic rings
Group D	4.4–6.0	Functional groups containing protons directly bonded to carbon atoms present in an aromatic ether molecule or carbon atoms present in carbohydrate-like molecules
Group E	6.0–8.0	Functional groups containing protons directly bonded to carbon atoms present in benzene-like structures
Group F	8.0–10.0	Functional groups containing protons directly bonded to carbon atoms present in aldehyde structures

suggest the presence of O–H containing molecules such as carboxylic acids, ketones and aldehydes [28, 29, 63]. The absence of major peaks transmittances from O–H stretching vibrations typically detected between wavenumbers of 3200 and 3600 cm^{-1} suggests the absence of water and other polymeric O–H compounds in the biocrude. Combining the NMR and the FTIR results presented so far, it is anticipated that the biocrude contains carboxylic acids, aromatic derivatives and nitrogenous compounds such as amides. The presence of these compounds will be further supported using the results of the gas chromatograph-mass spectrometry in the subsequent section.

3.2.3 Major chemical compounds detection by gas chromatograph-mass spectrometry

As presented in Table 4, the GC-MS assessment results indicate the presence of 11 *major* chemicals in the biocrude product. A comparative assessment of the composition of the biocrude product in the present study relative to the mean biocrude composition reported in previous studies is presented in Table 5. Table 4 shows that the three major chemicals present in the biocrude product are carboxylic acids and complex amides of octadec-9-enoic acid, n-hexadecanoic acid and n-Butylbenzenesulfonamide, with their percentage areas being 34.3%, 22.6% and 20.5%, respectively. The three major chemicals are formed due to the contribution of lipids and protein macromolecules, since carboxylic acids are generated from lipids and amides from proteins [66]. Table 5 shows that the percentage of aromatic compounds is within the range as reported in the literature. The generation of this aromatic amide shows that complex polymerisation reactions involving carbohydrate molecules occurred during the hydrothermal liquefaction process [67]. The results shown in Table 4 and Table 5 also indicate the absence of alkanes, aldehydes and phenolic compounds in the biocrude product in this study. The contribution of lipids to the biocrude product is further emphasised in Table 5 where it is shown that 74.1% of the major compounds in the biocrude are compounds containing the carboxylic group. The dominance of the lipid derivatives (carboxylic acids + esters) shown in Table 5 is also a reflection of the difference between the conversion efficiencies of macromolecules in hydrothermal liquefaction processes with lipids reported to have higher conversion efficiency than proteins, while proteins are reported to exhibit a higher conversion efficiency than carbohydrates [68].

Table 5 also shows that nitrogen-containing compounds are abundant in the biocrude product of the present study, with a contribution of 23% of the major chemicals detected. These nitrogen containing compounds include 2,5-Piperazinedione,3,6-bis(2-methylpropyl) and n-Butylbenzenesulfonamide with mole percentage of 2.5% and 20.5%, respectively. The presence of these nitrogen containing chemicals further demonstrates the contribution of proteins which are also responsible for the formation of nitrogenous compounds [68].

Although the TP of biocrude is shown to constitute a possible source of useful biochemicals, it is important that a cost-benefit assessment of introducing an additional catalytic hydrogenation step or undertaking complex compound recovery steps from the upgraded biocrude product is conducted. Such a cost-benefit assessment may constitute the basis of a future study.

3.2.4 Assessing the representative biocrude product as a liquid petroleum fuel alternative

The representative digestate biocrude is characterised by a HHV of 36.7 MJ/kg and an °API gravity value of 17.3. The values of the °API gravity and the HHV of the biocrude are shown to be within the range of values of the °API gravity and close to the HHV of heavy fraction of petroleum oil, which are 10 < °API gravity < 22.3 and 41.8 MJ/kg, respectively [69]. This suggests that the biocrude is quite similar to the heavy fraction of petroleum fuel. The results in this subsection

Table 3 Major functional groups and the associated compounds present in biocrude according to the FTIR results

Reference band (cm^{-1})	Wavenumber observed (cm^{-1})	Functional groups	Class of compounds
900–650	719, 891	O–H bending	Aromatic compounds
1300–950	1219, 1266	C–O stretching	Alcohol
1465–1350	1375, 1453	C–H bending	CH_3 and CH_2
1550–1490	1516	-NO_2 stretching	Nitrogenous compounds
1680–1580	1641	C=C stretching	Alkenes
1780–1640	1688	C=O stretching	Ketones, aldehydes, carboxylic acids
3000–2800	2922, 2844	C–H stretching	CH_3 and CH_2 (alkanes, carboxylic acids)
3600–3200	Negligible	O–H stretching	Polymeric O–H, water impurities

Table 4 Major compounds detected in digestate sourced representative biocrude product

Compound name	Chemical Abstracts Service Registry Number	Retention time (min)	Chemical formula	Molecular weight (kg/kmol)[a]	Normalised percentage (%) area[b]
Pterin-6-carboxylic acid	948-60-7	3.464	$C_7H_5N_5O_3$	207.1	3.2
Tetradecanoic acid	544-63-8	6.382	$C_{14}H_{28}O_2$	228.4	4.6
n-Butylbenzenesulfonamide	3622-84-2	6.748	$C_{10}H_{15}NO_2S$	213.3	20.5
Pentadecanoic acid	1002-84-2	7.300	$C_{15}H_{30}O_2$	242.4	1.6
3-Hydroxydodecanoic acid	1883-13-2	7.361	$C_{12}H_{24}O_3$	216.3	2.4
Oxiraneoctanoic acid, 3-octyl-, cis-	2566-91-8	7.452	$C_{18}H_{34}O_3$	298.5	4.1
1-docecanol,3,7,11- trimethyl-	56797-40-1	7.579	$C_{15}H_{32}O$	228.4	3
2,5-Piperazinedione,3,6-bis(2-methylpropyl)	1436-27-7	9.164	$C_{12}H_{22}N_2O_2$	226.3	2.5
n-Hexadecanoic acid	57-10-3	10.127	$C_{16}H_{32}O_2$	256.4	22.6
Benzyl (Z)-octadec-9-enoate	112-62-9	15.156	$C_{25}H_{40}O_2$	372.6	1.3
Octadec-9-enoic acid	112-80-1	16.391	$C_{18}H_{34}O_2$	282.5	34.3

[a,b] Area represents percent of the identified ion chromatograms [64]

therefore emphasise the possibility of employing biocrude as an alternative of heavy petroleum fuel.

Note however that the high oxygen content, 11.51 wt%, of the biocrude product compared to the mean oxygen content, 1 wt%, of petroleum crude [34] suggests that its direct utilisation as a petroleum refinery feedstock will present some challenges since such high oxygen content will promote the formation of undesirable emulsions in the petroleum refinery system [70]. This high oxygen content is also responsible for the lower HHV, 36.7 MJ/kg, of the biocrude compared to the mean HHV, 43 MJ/kg, of petroleum crude. It is therefore suggested that a further upgrading hydrogenation step is introduced to reduce the oxygen content and subsequently improve the HHV of the biocrude. The upgrading hydrogenation step is expressed by the following reaction [71]:

$$-(CH_2O)- + H_2 \rightarrow -(CH_2)- + H_2O \quad (6)$$

Table 5 Comparing the major chemicals present in typical hydrothermal liquefaction biocrude ;and the digestate-sourced biocrude

Compound categorisation	[a]Area %	[b]Area %
Phenolics	6–65	0
Esters	2–44	1.3
Aromatics and heterocyclics	6–35	31.6
Aldehydes	0–18	0
Carboxylic acids	2–40	74.1
Ketones	0–38	2.5
Alkanes	9–13	0
Nitrogen-containing compounds	12–23	23

[a,b] The present study []

where $-(CH_2O)-$ represents a representative oxygenated compound (i.e. n-hexadecanoic acid, $C_{16}H_{32}O_2$) in biocrude which can be upgraded to $-(CH_2)-$ (i.e. n-hexadecane, $C_{16}H_{34}$). Such a hydrogenation step will therefore facilitate the production of transportation-grade fuels.

3.2.5 Composition of the representative HTL-gas product

Employing the GC analysis methods described in methods section above, the composition of the HTL-gas product is presented in Table 6.

Table 6 shows that the HTL gas product contains a high molar fraction (87%) of CO2. Table 6, also shows that the combined mole fraction of CO and CO_2 constitutes about 91% of the HTL-gas product. This suggests that the dominant reactions responsible for the gas generation are decarbonylation (removal of CO) and decarboxylation (removal of CO_2) from the digestate. Also the poor yields of energy dense hydrocarbons such as C_2H_6, C_2H_4 and C_3H_8 suggests that engaging in further purification steps for useful hydrocarbon gas recovery will not constitute an economically viable process.

3.3 Representative biochar product as an agricultural soil additive

The poor HHV, 4.58 MJ/kg and the high ash content of the representative biochar product suggests that the utilisation of biochar as a solid fuel may not be considered as a viable approach with its alternative utilisation as a soil additive proposed. The results of other assessments, as a basis for an *initial and indicative measure* of biochar's viability as a soil additive, are therefore discussed below.

Table 6 Gaseous composition of the HTL gas

Gas components	Molecular formula	Mean mole percentage
Hydrogen	H_2	0.21
Carbon dioxide	CO_2	87.18
Methane	CH_4	0.42
Carbon monoxide	CO	4.03
Ethane	C_2H_6	0.03
Ethylene	C_2H_4	0.10
Propane	C_3H_8	0.38
Propene	C_3H_6	0.38
n-butane	C_4H_{10}	0.02
Trans-butene-2[a]	C_4H_8	0.30
Butene-1[a]	C_4H_8	6.63
Cis-butene-2[a]	C_4H_8	0.35

[a] Isomers

3.3.1 Thermal stability assessment

The comparative percentage changes in the mass of the biochar and in the mass of the dried digestate sample with increasing temperatures have been evaluated via a thermogravimetric analysis (TGA). The TGA results are depicted in Fig. 3. Figure 3 shows that the biochar is more thermally stable than the digestate, with the overall percentage loss in the masses of the biochar and digestate being 15.6% and 42.7%, respectively. Figure 3 also shows that the major mass loss of the digestate sample occurs at temperatures between 180 and 476 °C, with a total relative mass loss of 33%. This significant mass loss may be due to the thermal decomposition of anaerobic degradation-resistant hemicellulose, cellulosic and lignin in the digestate, since hemicellulose, cellulosic and lignin are thermally decomposed to gaseous components between 200 and 350 °C, between 300 and 430 °C and between 250 and 550 °C, respectively [72].

On the other hand, for the same temperature range of 180 to 476 °C, only 7.5% loss in the mass of the biochar was measured, highlighting the enhanced thermal stability of the biochar sample. Furthermore, a mass loss of only 2.4% was recorded between 30 and 257 °C for the biochar, compared to a mass loss of 9.13% measured between 257 and 484 °C, for a similar temperature change of 227 °C. This suggests that the rate of thermal decomposition of the biochar is enhanced at temperatures greater than ~257 °C. It is observed that for both biochar and digestate TGA plots, at temperatures between 500 and 680 °C, linear plots with a slope of approximately 0.03/°C for both samples are obtained. This suggests that mineralisation (or ashing), at temperatures above 500 °C, occurred at similar rates for both samples. Utilising Eq. 5 above the index of thermal lability (Th_l) of the biochar and digestate samples were also determined. Changes in mass of biochar between the temperature 110 and 350 °C ($\Delta m_{110–350°C}$) and between the temperature 350 and 550 °C ($\Delta m_{350–550°C}$) were calculated to be 0.461 mg and 1.038 mg, respectively. The changes in mass of digestate between the temperature 110 and 350 °C ($\Delta m_{110–350°C}$) and between the temperature 350 and 550 °C ($\Delta m_{350–550°C}$) were also calculated to be 3.174 mg and 1.969 mg, respectively. This implies that the Th_l of biochar and digestate are 0.44 and 1.61, respectively, indicating that biochar has an enhanced thermal stability of almost 4 times the thermal stability of the digestate. A careful consideration of the results will show that the ash content will have no influence on the Th_l results.

3.3.2 Morphological assessment

The morphologies of the dried digestate and biochar have been obtained and are shown in Fig. 4a–b. Figure 4 a shows that dried digestate exists as a homogenous structure with few surface pores. On the other hand, Fig. 4b shows that the morphology of the biochar is like a moulded skeleton having a significant number of pores and an uneven surface structure. The pores in the biochar may be due to the loss of residual volatiles originally present in the digestate. It is therefore clear that the introduction of the digestate to agricultural soil has the potential to improve the soil morphology of excessively compact soils by increasing overall soil porosity and reducing the

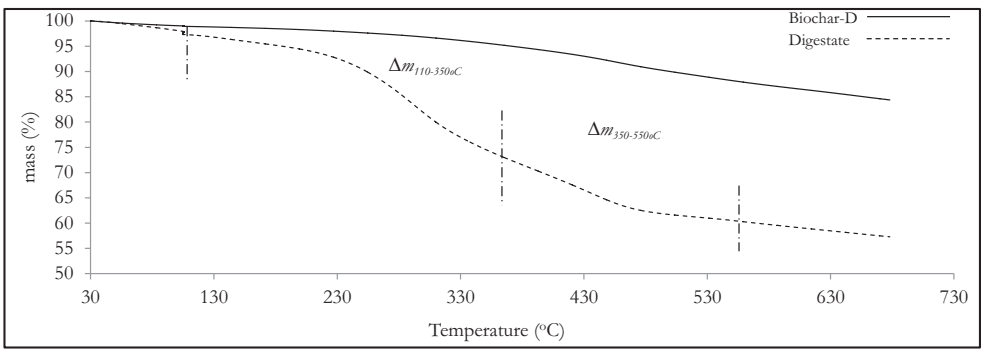

Fig. 3 Comparative TGA curves for HTL biochar and digestate

bulk density of soils. Such improvements in morphology will lead to improvements in water, heat and gas transfer within the soil [73].

3.3.3 The pH value and electrical conductivity of the representative biochar product

The pH and electrical conductivity (EC) of the biochar are presented and compared to the pH and EC of four biochars produced from other feedstocks (wood, bark, pea pod, orange leave) in Table 7. The pH value and the EC of the biochar in this study were determined to be 7.54 and 0.06 S/m, respectively. The pH values of the other biochars range from neutral to moderately alkaline and the value of EC of the other biochars ranging from 0.02–0.06 S/m. The pH value and the EC of the digestate in this study were determined to be 8.32 and 0.57 S/m, respectively, which are not shown in Table 7.

The introduction of biochars characterised with pHs ranging from highly alkaline to moderately alkaline may serve to improve soil performance. This is because acidic soils may limit the bioavailability of plant nutrients and thus negatively influence plant growth [47]. Current practice in most developed countries requires that the acidity challenge of soils is resolved via the introduction of lime which is a conventional soil acidity neutraliser. However, the use of lime leads to several undesirable effects such as the $CaCO_3$ formation reactions which may lead to soil pulverisation and depletion of calcium ions availability in soils [76]. Given that the biochar product is only slightly alkaline as shown in Table 7, the neutralisation of acidic soils may require the introduction of significant masses of the biochar product for any noticeable improvement in the soil pH value to be observed.

Initial considerations may suggest that the more alkaline digestate may constitute a more useful input to soils if the neutralisation of soil acidity constitutes the *major* and *only* concern since the digestate is clearly more alkaline than the biochar, as illustrated by its higher pH value of 8.32 relative to the pH value of biochar of 7.54. However, one benefits of using biochar compared to using digestate irrespective of its lower pH value is that the cost of raw digestate treatment for biochar production process via HTL is considerably cheaper than the raw digestate treatment process for sterilised digestate production as discussed earlier above. Furthermore, soil additives characterised by pH values closer to neutrality (i.e. pH close to 7) and high number of pores ("situation A")are preferred to soil additives characterised by a strongly alkaline pH value and lower number of pores ("situation B") [77]. This is because "situation A" presents a scenario where the soil additive has additional benefits of constituting a better adsorbent for any contaminants present agricultural soils compared to "situation B". This implies that the introduction of the slightly alkaline biochar (pH, 7.54) from the HTL of digestate as a soil additive has the potential of not only enhancing the transfer of useful nutrients and water due to its high number of pores but also facilitating a reduction of the bioavailability of contaminants in soils more efficiently than the alternative more alkaline digestate. The electrical conductivity (EC) of soils is considered as an important indicator of soil health since it reflects the availability of nutrients such nitrogen for plant growth [48]. Soil characterised by low EC values, such as sandy soils having EC values as low as 5 μS/c [78], are therefore considered as low-quality soils. Given that the mean EC value of the biochar is measured to be 0.06 S/m, it suggests that the introduction of the biochar to low-quality soils has the potential of imporving the overall EC value of poor soils.

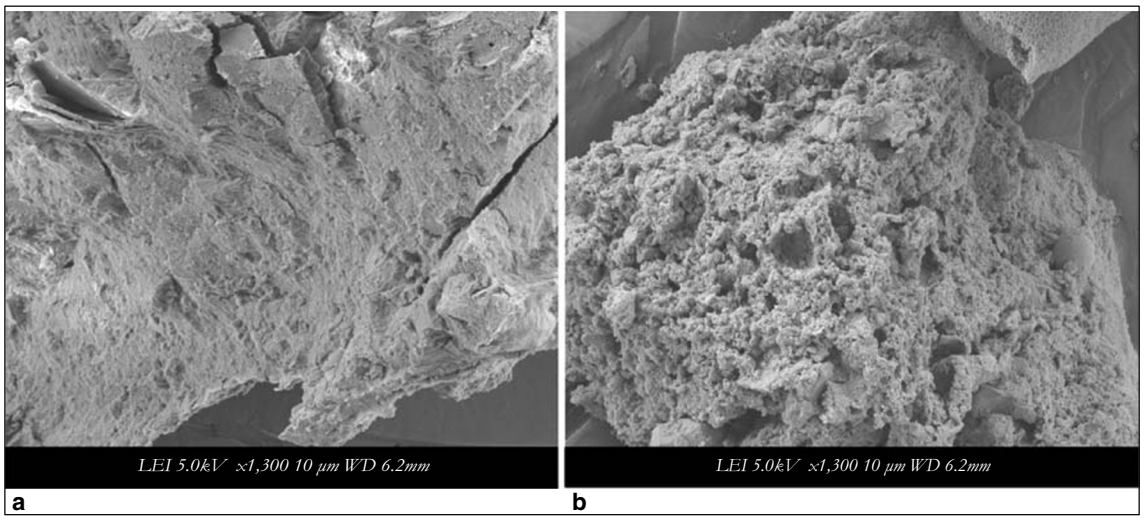

Fig. 4 Morphological changes in the digestate before [a] and after [b] hydrothermal liquefaction processing

Table 7 The pH value and the EC of the digestate

Determined properties	Biochar-wood[a]	Biochar-bark[a]	Biochar-pea pod[b]	Biochar-orange leave[b]	TP of Biochar[c]
pH	7.56	9.84	8.84	9.43	7.54
EC (S/m)	0.02	0.13	0.06	0.02	0.06

[a,b,c] This study, i.e. digestate-HTL biochar [74, 75]

3.3.4 Mineral content of the representative biochar

The mineral content of biochar has been measured. Table 8 therefore highlights the mean concentrations of the major nutrients of nitrogen, potassium, phosphorous, calcium, magnesium sulphur, iron, manganese, zinc, nickel, copper, sodium, titanium, aluminium and boron in the biochar.

Comparing the mineral content of the biochar to the minimum mineral requirements necessary for crop growth as specified by Epstein [79], it may be seen that if the minerals present in biochar are *available* for crop use, biochar has the potential to serve as a rich source of minerals. Utilising a similar argument, the high concentration of aluminium in biochar, measured to be 77.500 g/kg, highlights the risk of aluminium toxicity to plants when introduced to soils [58].

It must however be acknowledged that aluminium toxicity is only manifested in acidic soils characterised with pH values of below 5.0 [80], since under such acidic conditions, the phytotoxic form of aluminium, namely, its Al^{3+} ionic form, predominates [58]. This suggests that since the biochar (slightly alkaline) will serve to increase the pH of soils, its introduction to acidic soils may not lead to aluminium toxicity effects since the introduction of the biochar to the soil will make it less acidic. Indeed, small increments in the pH value are shown to be capable of reducing plant accessibility to the unwanted phytotoxic aluminium form of Al^{3+} [58, 80].

As stated earlier above, the current study acknowledges that the high mineral content of biochar does not translate to mineral availability in soils for crop growth; this study however demonstrates the presence of some useful nutrients in the biochar product from the HTL of digestate that may be potentially available for plant use.

Table 8 Mineral content of the biochar product

Mineral	Mean biochar nutrient content (g/kg)
Nitrogen	8.850
Potassium	16.500
Phosphorous	40.500
Calcium	71.900
Magnesium	11.000
Sulphur	3.350
Iron	28.000
Manganese	0.960
Zinc	1.109
Nickel	0
Copper	415.000
Boron	0
Sodium	8.150
Titanium	3.630
Aluminium	77.5

4 Conclusion

This paper has explored the application of the products of hydrothermal liquefaction of digestate for practical uses. It has been demonstrated that the hydrothermal liquefaction technology facilitates the generation of useful biocrude and biochar products which can serve as a possible liquid biofuel or crude biochemical mixture and a soil additive, respectively. The higher heating value of the biocrude product of 36.7 MJ/kg suggests that it may serve as an energy dense fuel. Its similarity to the heavy fraction of petroleum crude was also highlighted. The compositional analyses of the biocrude product using NMR, FTIR and GC-MS methods have demonstrated the dominant presence of amides and fatty acid compounds in the biocrude. On the other hand, the poor higher heating value 4.58 MJ/kg of the typical product of biochar suggests that its preferred utilisation as a possible agricultural soil enhancer since it is not logical to employ the biochar as a solid fuel from an energetic perspective. Some agronomic properties of the biochar such as morphology, pH value, electrical conductivity, mineral content and thermal stability have been investigated experimentally, and these properties have been shown to highlight the potential use of biochar as an agricultural soil additive.

Acknowledgements Special thanks are expressed to Pauline Bandeen and Lisa Bucke of the Micro analytical laboratory of the Department of Chemistry, University of Otago, New Zealand, Ian Stewart also of the Department of Chemistry, University of Otago, New Zealand and Ashley Duncan of the Department of Human Nutrition, University of Otago for the use of their facilities for the analysis of samples.

References

1. Okoro OV, Sun Z, Birch J (2018) Prognostic assessment of the viability of hydrothermal liquefaction as a post-resource recovery step after enhanced biomethane generation using co-digestion technologies. Appl Sci 8(11):https://doi.org/10.3390/app8112290
2. Okoro OV, Sun Z, (2019) Desulphurisation of Biogas: A Systematic Qualitative and Economic-Based Quantitative Review of Alternative Strategies. Chem Eng 3 (3):76
3. Logan M, Visvanathan C, (2019) Management strategies for anaerobic digestate of organic fraction of municipal solid waste: Current status and future prospects. Waste Manag & Res 37 (1_suppl):27-39
4. Baggesen DL (2007) Veterinary safety in relation to handling of manure and animal by products and the use of biogas technologies. In: Presentation National Food Institute Denmark
5. Hentges DJ (1996) Anaerobes: general characteristics. In: medical microbiology. 4th edition. University of Texas Medical Branch at Galveston, Galveston, Texas
6. Okoro OV, Sun Z, Birch J (2017) Meat processing waste as a potential feedstock for biochemicals and biofuels – a review of possible conversion technologies. J Clean Prod 142(part 4):1583–1608
7. Golkowska K, Vázquez-Rowe I, Lebuf V, Accoe F, Koster D (2014) Assessing the treatment costs and the fertilizing value. Water Sci Technol 69(3):656–662
8. Okoro OV, Zhifa S, Birch J (2019) Thermal depolymerization of biogas digestate as a viable digestate processing and resource recovery strategy. In: Advances in Eco-Fuels for a Sustainable Environment. Wood head publishing Cambridge, pp 277–308
9. Okoro OV, Sun Z, Birch J (2018) Thermal depolymerisation of digestate for biofuel and biomaterial production. In Proceedings of the 2014th World Congress on New Technologies (NewTech'2018), Madrid, Spain, pp 2019-2021
10. Biller P, Lawson D, Madsen RB, Becker J, Iversen BB, Glasius M (2017) Assessment of agricultural crops and natural vegetation in Scotland for energy production by anaerobic digestion and hydrothermal liquefaction. Biomass Conv Bioref 7:467–477
11. Vardon DR, Sharma BK, Scott J, Yu G, Wang Z, Schideman L, Zhang Y, Strathmann TJ (2011) Chemical properties of biocrude oil from the hydrothermal liquefaction of Spirulina algae, swine manure, and digested anaerobic sludge. Bioresour Technol 102(17):8295–8303
12. ASTM (1998) D2017–98 Standard test method of accelerated laboratory test of natural decay resistance of woods , decay, evaluation, laboratory, natural, resistance and subjected to termite bioassay according to no-choice test procedure based upon AWPA E1–97 (AWPA, 1. West Conshohocken
13. IBI (2012) IBI biochar standard. Minesota
14. Domingues RR, Trugilho PF, Silva CA, de Melo ISNA, Melo LCD, Magriotis ZA, Sánchez-Monedero MA (2017) Properties of biochar derived from wood and high-nutrient biomasses with the aim of agronomic and environmental benefits. PLoS One 12(5): e0176884. https://doi.org/10.1371/journal.pone.0176884
15. ASTM (2015) ASTM D3176–15 Standard practice for ultimate analysis of coal and coke. ASTM International, West Conshohocken
16. Channiwala SA, Parikh PP (2002) A unified correlation for estimating HHV of solid, liquid and gaseous fuels. Fuel 81:1051–1063
17. Gai C, Zhang Y, Chenb W, Zhang P, Donga Y (2014) Energy and nutrient recovery efficiencies in biocrude oil produced via hydrothermal liquefaction of Chlorella pyrenoidosa. RSC Adv 4:16958–16967
18. Barnés MC, de Visser MM, Rossum GV, .Kersten SRA, Lange JP (2017) Liquefaction of wood and its model components. J Anal Appl Pyrolysis 125:136–143
19. Wu Z, Rodgers RP, Marshall AG (2004) 2 and 3-dimensional van Krevelen Diagrams: a graphical analysis complementary to the Kendrick mass plot for sorting elemental compositions of complex organic mixtures based on ultrahigh-resolution broadband Fourier transform ion cyclotron resonance mass. Anal Chem 76(9):2511–2516
20. Fryda L, Visser R (2015) Biochar for soil improvement: evaluation of biochar from gasification and slow pyrolysis. Agriculture 5(4): 1076–1115
21. Luo L, Sheehan JD, Dai L, Savage PE (2016) Products and kinetics for isothermal hydrothermal liquefaction of soy protein concentrate. ACS Sustain Chem Eng 4:2725–2733
22. Chen W-T, Zhang Y, Zhang J, Yu G, Schideman LC, Zhang P, Minarick M (2014) Hydrothermal liquefaction of mixed culture algal biomass from wastewater treatment system into biocrude oil. Bioresour Technol 152:130–139
23. Vardon DR, Sharma BK, Blazina GV, Rajagopalan K, Strathmann TJ (2012) Thermochemical conversion of raw and defatted algal biomass via hydrothermal liquefaction and slow pyrolysis. Bioresour Technol 109:178–187
24. Chen W-T, Zhang Y, Zhang J, Yu G, Schideman LC, Zhang P et al (2014) Co- liquefaction of swine manure and mixed- culture algal biomass from wastewater treatment system to produce biocrude oil. Appl Energy 128:209–216
25. Mullen CA, Strahan GD, Boateng AA (2009) Characterization of various fast-pyrolysis bio-oils by NMR spectroscopy. Energy Fuel 23:2707–2718
26. Özbay N, Apaydın-Varol E, Uzun BB, Pütün AE (2008) Characterization of bio-oil obtained from fruit pulp pyrolysis. Energy 33:1233–1240
27. Cheng F, Cui F, Chen L, Jarvis J, Paz N, Schaub T, Nirmalakhandand N, Brewera CE (2017) Hydrothermal liquefaction of high- and low-lipid algae: bio-crude oil chemistry. Appl Energy 206:278–292
28. Qian Y, Zuo C, Tan J, He J (2007) Structural analysis of bio-oils from sub-and supercritical water liquefaction of woody biomass. Energy 32(3):196–202
29. Zhang L, Shen C, Liu R (2014) GC–MS and FT-IR analysis of the bio-oil with addition of ethyl acetate during storage. Front Energy Res. https://doi.org/10.3389/fenrg.2014.00003
30. Jena U, Das KC (2011) Comparative evaluation of thermochemical liquefaction and pyrolysis for bio-oil production from microalgae. Energy Fuel 25:5472–5482
31. Li H, Yuan X, Zeng G, Huang D, Huang H, Tong J, You Q, Zhang J, Zhou M (2010) The formation of bio-oil from sludge by deoxy-liquefaction in supercritical ethanol. Bioresour Technol 101:2860–2866
32. Karagöz S, Bhaskar T, Muto A, Sakata Y (2005) Comparative studies of oil compositions produced from sawdust, rice husk, lignin and cellulose by hydrothermal treatment. Fuel 84:875–884
33. Chumpoo J, Prasassarakich P (2010) Bio-oil from hydro-liquefaction of bagasse in supercritical ethanol. Energy Fuel 24: 2071–2077
34. API (2011) Crude oil: CAS No. 8002-05-9. American Petroleum Institute, Washington D.C.
35. Flagan RC, Seinfeld JH (1988) Combustion fundamentals. In: Fundamentals of air pollution engineering. Prentice-Hall, Englewood Cliffs, pp 59–166

36. Demirbas A (2002) Relationships between heating value and lignin, moisture, ash and extractive contents of biomass fuels. Energy Explor Exploit 20:105–111
37. Al-arenan S, Alkathiri N, Al-Rashed Y, Doshi T, Alfawzan Z, Six S, Yermankov V (2016) GCC-NEA oil trade: competition in asian oil markets and trhe Russian 'pivot' east in: energy relations and policy making in Asia. Springer, Singapore
38. Makinde I, Lee WJ (2016) Reservoir simulation models – impact on production forecasts and performance of shale volatile oil reservoirs. Glob J Res Eng Gen Eng 16(4):53–69
39. Kayan C (2012) Systems of units: National and International Aspects. Literary Licensing, Califonia
40. Campbell J (2014a) Simple equations to approximate changes to the properties of crude oil with changing temperature. https://www.petroskills.com/blog/entry/crude-oil-and-changing-temperature#.XeEP4Ogzbcs/. Accessed 2 Nov 2018
41. ASTM (2013) Standard test method for specific gravity and density of semi-solid bituminous materials (Pycnometer Method)ASTM D70–03 American Society for Testing and Materials International, West Conshohocken
42. Chintala R, Mollinedo J, Schumacher TE, Malo DD, Julson JL (2014) Effect of biochar on chemical properties of acidic soil. Arch Agron Soil Sci 60:393–404
43. Thies JE, Rillig MC (2009) Characteristics of biochar: biological properties (Ch. 6). In: Biochar for environmental management. Earthscan, Gateshead, pp 85–105
44. Rutherford DW, Wershaw RL, Rostad CE, Kelly CN (2012) Effect of formation conditions on biochars: compositional and structural properties of cellulose, lignin, and pine biochars. Biomass Bioenergy 46:693–701
45. Vantieghem S (2016) Carbon dioxide sequestration by means of biochar: analytical pyrolysis as a stability proxy method. Faculty of Bioscience Engineering: Gent University Gent
46. Jindo K, Sonoki T, Matsumoto K, Canellas L, Roig A, Sanchez-Monedero MA (2016) Influence of biochar addition on the humic substances of composting manures. Waste Manag 49:545–552. https://doi.org/10.1016/j.wasman.2016.01.007
47. Goulding KWT (2016) Soil acidification and the importance of liming agricultural soils with particular reference to the United Kingdom. Soil Use Manag 32:390–399
48. Carmo DL, Silva CA, Lima JM, Pinheiro GC (2016) Electrical conductivity and chemical composition of soil solution: comparison of solution samplers in tropical soils. Rev Bras Ciênc Solo 40: e0140795
49. IBI (2015) IBI Biochar Standards Version 2.0. International biochar initiative, US
50. Lenntech (2019) Water conductivity. In: https://www.lenntech.com/applications/ultrapure/conductivity/water-conductivity.htm./. Accessed 11 Oct 2018
51. Filiberto DM, Gaunt JL (2013) Practicality of biochar additions to enhance soil and crop productivity. Agriculture 3(4):715–725
52. Nair VD, KR NP, Dari B, Freitas AM, Chatterjee N, Pinheiro FM (2017) Biochar in the agroecosystem–climate-change–sustainability nexus. Front Plant Sci 8.https://doi.org/10.3389/fpls.2017.02051
53. Asad A, Rafique R (2000) Effect of zinc, copper, iron, manganese and boron on the yield and yield components of wheat crop in tehsil Peshawar. Pak J Biol Sci 3(10):1615–1620
54. Burton LD (2009) Agriscience fundamentals and applications, 5th edn. Cengage learning, New York
55. Subbarao GV, Ito O, Berry WL, Wheeler RM (2003) Sodium—a functional plant nutrient. Crit Rev Plant Sci 22(5):391–416
56. Lyu S, Wei X, Chen J, Wang C, Wang X, Pan D (2017) Titanium as a beneficial element for crop production. Front Plant Sci 8:597. https://doi.org/10.3389/fpls.2017.00597
57. Bojórquez-Quintal E, Escalante-Magaña C, Echevarría-Machado I (2017) Aluminum, a friend or foe of higher plants in acid soils. Front Plant Sci 8. https://doi.org/10.3389/fpls.2017.01767
58. Rout G, Samantaray S, Das P (2001) Aluminium toxicity in plants: a review. Agronomie, EDP Sciences 21(1):3–21
59. EIA (2017) distillate fuel oil U.S. Energy Information Administration, Washinton D.C.
60. Apex (2015) FUEL OIL NO. 6, Safety Data Sheet. Apex oil company Inc., Missouri
61. Gaur S, Reed TB (1998) Thermal data for natural and synthetic fuels. Marcel Dekker, New York
62. Okoro OV, Sun Z, Birch J (2017) Meat processing dissolved air flotation sludge as a potential biodiesel feedstock in New Zealand: a predictive analysis of the biodiesel product properties. J Clean Prod 168:1436–1447
63. Feng S, Yuan Z, Leitch M, Xu CC (2014) Hydrothermal liquefaction of barks into bio-crude – effects of species and ash content/composition. Fuel 116(15):214–220
64. Webbook NC (2016) NIST standard reference database number 69. NIST, USA
65. Ramirez JA, Brown RJ, Rainey TJ (2015) A review of hydrothermal liquefaction bio-crude properties and prospects for upgrading to transportation fuels. Energies 8:6765–6794
66. Wu Y, Chen Y, Wu K (2014) Role of co-solvents in biomass conversion reactions using sub/ supercritical water. In: Near-critical and supercritical water and their applications for biorefineries. Springer, New york, pp 69–98
67. Zhang C, Tang X, Sheng L, Yang X (2016) Enhancing the performance of Co-hydrothermal liquefaction for mixed algae strains by the Maillard reaction. Green Chem 18 (8):2542–2553
68. Biller P, Ross AB (2011) Potential yields and properties of oil from the hydrothermal liquefaction of microalgae with different biochemical content. Bioresour Technol 102(1):215–225
69. EngineeringToolBox (2003) Fuels - Higher and Lower Calorific Values In: Engineering ToolBox. https://www.engineeringtoolbox.com/fuels-higher-calorific-values-d_169.html/. Accessed 13 Nov 2018
70. Strezov V, Evans TJE (2015) Biomass processing technologies. CRC Press, Boca Raton
71. Demirbas A (2011) Competitive liquid biofuels from biomass. Appl Energy 88:17–28
72. Mohammad IJ, Mohammad GR, Ashfaque AC, Ashwath N (2012) Biofuels production through biomass pyrolysis—a technological review. Energies 5:4952–5001
73. Blanco-Canqui H (2017) Review & Analysis–Soil Physics & hydrology: biochar and soil physical properties. Soil Sci Soc Am J 81: 687–711
74. Buss W (2016) Contaminant issues in production and application of biochar. The University of Edinburgh, Edinburgh
75. Stella MG, Sugumaran P, Niveditha S, Ramalakshmi B, Ravichandran P, Seshadri S (2016) Production, characterization and evaluation of biochar from pod (Pisum sativum), leaf (Brassica oleracea) and peel (Citrus sinensis) waste. Int J Recycl Org Waste Agric 5:43–53
76. Umesha T, Dinesh S, Sivapullaiah P (2009) Control of dispersivity of soil using lime and cement. Int J Geol 3(1):8–16
77. Nartey OD, Zhao B (2014) Biochar preparation, characterization, and adsorptive capacity and its effect on bioavailability of contaminants: an overview. Advances in Materials Science and Engineering 2014. https://doi.org/10.1155/2014/715398

78. Barbosa RN, Overstreet C (2011) What is soil electrical conductivity LSU AgCenter pub. 3185, Los Angeles
79. Epstein E (1965) Mineral metabolism. In: Plant biochemistry. Wiley, New York, pp 438–466
80. Yang M, Tan L, Xu Y, Zhao Y, Cheng F, Ye S, Jiang W (2015) Effect of low pH and aluminum toxicity on the photosynthetic characteristics of different fast-growing eucalyptus vegetatively propagated clones. PLoS One 10(6):e0130963. https://doi.org/10.1371/journal.pone.0130963